MODELLING AND FILTERING ALMOST PERIODIC SIGNALS BY TIME-VARYING FOURIER SERIES WITH APPLICATION TO NEAR-INFRARED SPECTROSCOPY

Ivo Trajkovic[13], *Christoph Reller*[2], *Martin Wolf*[3], *Hans-Andrea Loeliger*[2]

[1] Dept. ITET, ETH Zurich, Switzerland, trajkovic@biomed.ee.ethz.ch
[2] Dept. ITET, ETH Zurich, {reller, loeliger}@isi.ee.ethz.ch
[3] Dept. Obstetrics, University Hospital Zurich, {ivo.trajkovic, martin.wolf}@usz.ch

ABSTRACT

We propose a new approach to modelling almost periodic signals and to model-based estimation of such signals from noisy observations. The signal model is based on Fourier series where both the coefficients and the fundamental frequency can continuously change over time. This signal model can be represented by a factor graph which we use to derive message passing algorithms to estimate the time-dependent model parameters from the observed samples.

Our motivating application is near-infrared spectroscopy. In this application the observed signal is a superposition of several physiological signals of clinical interest (including, in particular, the arterial pulsation), and we wish to decompose the observed signal into these components. Most of these component signals are almost periodic. We show that the proposed algorithm can be used to extract the arterial pulsation from the measured signal.

1. INTRODUCTION

Many signals in nature are almost periodic. In this paper, we propose a new approach to modelling and to model-based estimation of such signals. Our immediate motivation comes from near-infrared spectroscopy (NIRS), where the observed signals typically look as in Fig. 1. The main feature in Fig. 1 is the arterial pulsation (the heartbeat), which is almost periodic (with a period of about 100 samples in this example). The challenge is to extract the "clean" arterial pulsation and to subtract it from the observed signal in order to make the residual signal available for further analysis (see Section 2). Note that, because of the sharp peaks of the pulses, a simple low-pass filter will not do.

Recall that a periodic signal can be represented by a Fourier series. Specifically, let $x_1, x_2, \ldots$ be the sampled version (with equidistant samples) of a periodic real-valued signal. Then we can write

$$x_n = \mathrm{Re}\left(\sum_{k=0}^{\infty} A_k e^{jkn\Omega}\right) \tag{1}$$

with real coefficient A_0, with complex coefficients $A_1, A_2, \ldots$, and with fundamental frequency $\Omega \in \mathbb{R}$. We now propose to model almost periodic signals by changing (1) to

$$x_n = \mathrm{Re}\left(\sum_{k=0}^{K} A_{k,n} e^{jk\Theta_n}\right) \tag{2}$$

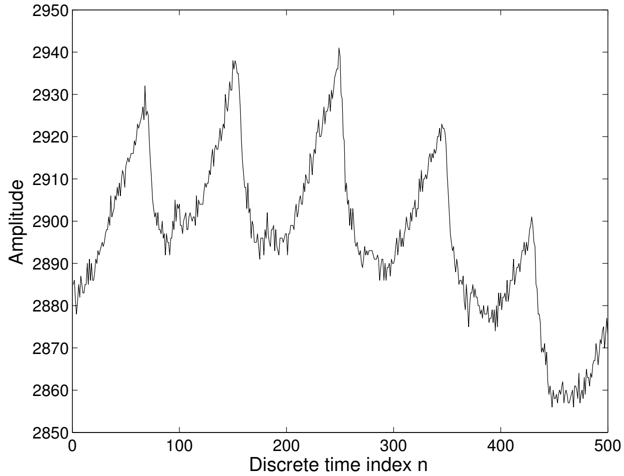

Figure 1: A measured NIRS signal with about five periods of the arterial pulsation.

with

$$A_{k,n+1} \approx A_{k,n} \tag{3}$$

and

$$\Theta_{n+1} = (\Theta_n + \Omega_n) \bmod 2\pi \tag{4}$$

with

$$\Omega_{n+1} \approx \Omega_n. \tag{5}$$

Note also that (i) we restrict ourselves to a finite number K of frequencies in (2), (ii) we allow the fundamental frequency to continuously change over time, thus Ω is replaced by the time-dependent parameter Ω_n implying that $n\Omega$ in (1) is replaced by the parameter Θ_n, from now on called *phase*, and the relation (4) between two temporal consecutive phases is imposed, (iii) we allow the coefficients to continuously change over time, thus the fixed coefficients A_k in (1) are replaced by the time-dependent coefficients $A_{k,n}$. The meanings of (3) and (5) are not formally defined here. These constraints are, however, motivated through the fact that the period length and signal shape, e.g. the heart rate and the beat shape in the arterial pulsation, slightly vary.

Now let $y_1, y_2, \ldots$ be a noisy version of the signal $x_1, x_2, \ldots$. Specifically,

$$y_n = x_n + Z_n \tag{6}$$

where $Z_1, Z_2, \ldots$ is discrete-time white Gaussian noise. The main point of this paper is that the parameters $A_{k,n}$ and Θ_n (for $k = 0, 1, \ldots, K$ and for $n = 1, 2, 3, \ldots, N$) can be efficiently estimated from $\boldsymbol{y} = (y_1, \ldots, y_N)$ with a complexity that is linear both in K and in N. An estimate of the "clean" signal $\boldsymbol{x} = (x_1, \ldots, x_N)$ may then be obtained from (2).

The proposed approach may be outlined as follows. First, equations (2)–(6) can be turned into a state space model that can be represented by a factor graph [1, 2]. We then use message passing algorithms in this factor graph to estimate all the parameters. The estimates are optimal in the least-squares sense, i.e. they result in minimal

$$\sum_{n=1}^{N} (y_n - x_n)^2.$$

The soft constraint in (3) is handled with adjustable strength by message damping, as will be described in Section 3.4 ("$\overset{\gamma}{=}$"-node). The soft constraint in (5) is handled with adjustable strength by using prior knowledge about the upper and lower limits of Ω_n, as will be described in Section 3.3 ("$\mathcal{I}$"-node).

In contrast to other well-known methods, like Independent Component Analysis (ICA) described in [3] or the traditional bandpass filtering used in [4], our method allows explicit modelling of the almost periodic signal resulting in adaptive filtering. A different adaptive filter, presented in [5], Section 6.5.2, finds an average shape by matching all periods in the arterial pulsation of a long NIRS measurement in one subject. This shape comprises periodicity in the arterial pulsation. The disadvantages of this filter compared to our filter are: (i) it needs a large observation dataset, and (ii) it assumes for every period the same shape, which is unrealistic.

The next section of this paper is about NIRS and shows some experimental results with the proposed algorithm. The algorithm itself is described in Section 3.

2. APPLICATION TO NEAR-INFRARED SPECTROSCOPY

NIRS was described in detail in [5], [6], and [7]. Our experimental data was obtained by the equipment developed and described in [5]. Light from a suitable source is sent through some tissue, where it is scattered and absorbed. Some of the light finds its way to the detector. In living tissue, the intensity of the detected light varies due to a number of physiological effects reflected in the blood [8]. We here assume that the intensity of the detected light is a linear superposition of several component signals including the arterial pulsation (due to the heartbeat), the respiration, slow oscillations, etc., most of which are almost periodic. We wish to decompose the measured signal (the light intensity) into these component signals, all of which are of clinical interest. In particular, we wish to extract the arterial pulsation and subtract it from the measured signal in order to make the residual signal available for further analysis.

Some results with the proposed new method are shown in Fig. 2. Many more experimental results are now available which confirm the validity of the proposed method. This means that our approach will improve the diagnosis capabilities and extend the area of application of NIRS.

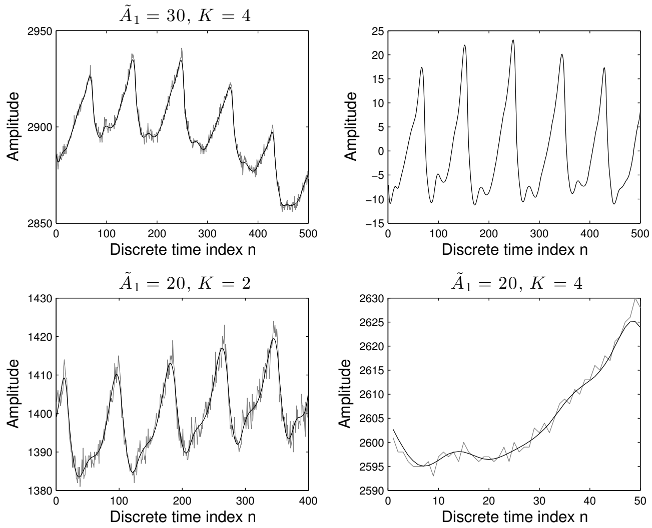

Figure 2: Examples of measured NIRS observations (noisy curves) with sampling frequency $f_s = 100$ Hz and corresponding estimated signals (smooth curves). The top right plot shows the estimated arterial pulsation of the signal in the top left plot, which is obtained by subtracting the DC coefficient estimates $(\hat{A}_{0,1}, \ldots, \hat{A}_{0,N})$ from the estimated signal (the smooth curve) in the top left plot. The bottom left plot shows that the algorithm works for observations with rather strong noise. The bottom right plot shows that it also works for short observation datasets (50 samples). In all these examples, the damping parameter γ (see Section 3.4) was $\gamma = 0.96$, and convergence was achieved in 3 iterations.

3. ESTIMATING THE MODEL PARAMETERS

The estimation of the model parameters is structured into several blocks, as will be described in Section 3.1. The factor graphs of the two main blocks will be introduced in Section 3.2, and the corresponding message passing algorithms will be described in Sections 3.3 and 3.4.

3.1 The Building Blocks of the Estimation Algorithm

Given a set of N observed (measured) samples $\boldsymbol{y}$, the objective is to estimate the model parameter vector $\boldsymbol{\Theta} \triangleq (\Theta_1, \ldots, \Theta_N)$ and coefficient matrix

$$\mathbf{A} = \begin{pmatrix} A_{0,1} & \ldots & A_{0,N} \\ \vdots & \ddots & \vdots \\ A_{K,1} & \ldots & A_{K,N} \end{pmatrix}$$

and reconstruct the almost periodic signal by applying the estimates in (2). We will use $\boldsymbol{A_{k,-}}$ for the k-th row and $\boldsymbol{A_{-,n}}$ for the n-th column of $\mathbf{A}$.

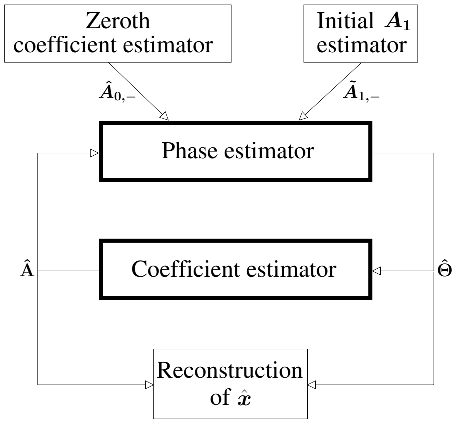

Figure 3: The building blocks of the estimation algorithm.

We propose an iterative, parameter-wise maximum a-posteriori estimation procedure. Based on the observation dataset $\boldsymbol{y}$ and a given estimate $\hat{\mathbf{A}}$ of $\mathbf{A}$ we make estimates $\hat{\Theta}_n$ of Θ_n as

$$\hat{\Theta}_n = \underset{\Theta_n \in [0,2\pi]}{\arg\max}\, f\Big(\Theta_n \;\Big|\; \boldsymbol{y}, \hat{\mathbf{A}}\Big), \tag{7}$$

where the conditional probability density function f in (7) comprises the model (2), the relation (4) and the constraint (5), which is handled with adjustable strength by using prior knowledge about the upper and lower limits of Ω_n, as will be described in Section 3.3 ("$\mathcal{I}$"-node).

Likewise we make estimates $\hat{A}_{k,n}$ of $A_{k,n}$ based on the observation dataset $\boldsymbol{y}$, estimates $\hat{A}_{k-1,1}, \ldots, \hat{A}_{k-1,N}, \ldots, \hat{A}_{0,1}, \ldots, \hat{A}_{0,N}$, and $\hat{\boldsymbol{\Theta}}$ from the previous iteration step as

$$\begin{aligned}\hat{\boldsymbol{A}}_{k,n} = \underset{A_{k,n} \in \mathbb{C}}{\arg\max}\, & f(A_{k,n} \mid \boldsymbol{y}, \hat{A}_{k-1,1}, \ldots, \\ & \hat{A}_{k-1,N}, \ldots, \hat{A}_{0,1}, \ldots, \hat{A}_{0,N}, \hat{\boldsymbol{\Theta}})\end{aligned} \tag{8}$$

for increasing k. The function f in (8) comprises the model (2) and the constraint (3), which is handled with adjustable strength by message damping, as will be described in Section 3.4 ("$\overset{\gamma}{=}$"-node).

The whole estimation algorithm is split into several building blocks. One block produces the coefficient estimates $\hat{\boldsymbol{A}}_{\mathbf{0},-}$, a second block produces the initial estimate $\tilde{\boldsymbol{A}}_{\mathbf{1},-}$. The two main blocks produce the coefficient estimate matrix $\hat{\mathbf{A}}$ and the phase estimate vector $\hat{\boldsymbol{\Theta}}$. The last block reconstructs the almost periodic signal $\hat{\boldsymbol{x}}$. The interaction between these blocks is depicted in Fig. 3.

The coefficient estimator normally uses the estimates produced by the phase estimator block and vice versa. In the beginning, however, the zeroth coefficient estimator independently estimates the DC component $\hat{\boldsymbol{A}}_{\mathbf{0},-}$ by means of (8). Since for this there is no need for $\hat{\boldsymbol{\Theta}}$, this is a one-time procedure based on the observation $\boldsymbol{y}$ only. It can be shown that for this case (8) boils down to a first-order low-pass filter. The estimates are then fed to the phase estimator block together with an initial estimate $\tilde{\boldsymbol{A}}_{\mathbf{1},-}$. In almost periodic signals measured with NIRS, most of the signal energy, apart from the DC component $\boldsymbol{A}_{\mathbf{0},-}$ and the noise, lies in the fundamental frequency component $\boldsymbol{A}_{\mathbf{1},-}$. Therefore, when applying our algorithm to NIRS, a first rough estimate of the almost periodic signal is simply a sinusoid. Its magnitude $\tilde{\boldsymbol{A}}_{\mathbf{1},-}$ is calculated by the initial A_1 estimator block in such a way that the sinusoid is of the same energy as the signal $\boldsymbol{y} - \hat{\boldsymbol{A}}_{\mathbf{0},-}$. Based on this estimate the phase estimator is already able to produce a good estimate $\hat{\boldsymbol{\Theta}}$. The latter is handed over to the coefficient estimator, which finally calculates the full set of coefficient estimates $\hat{\mathbf{A}}$.

At this point it is possible to apply entries of $\hat{\boldsymbol{\Theta}}$ and columns of $\hat{\mathbf{A}}$ directly in (2) and get a first estimate $\hat{\boldsymbol{x}}$ of the almost periodic signal. The result can, however, be improved by iterating a few times.

3.2 Factor Graphs for the Main Building Blocks

The estimations are done by using the sum-product message passing algorithm on factor graphs, which is described in detail in [2].

By using a Fourier series as the model where both the coefficients and the fundamental frequency are time-dependent, the message passing algorithm can be regarded as matching, in the least-squares sense, a sliding discrete-time Fourier series with the observation.

Message passing is applied on the factorial temporal decomposition of the statistical model called factor graph (see [1], Chapter 2). With respect to (2)–(6) a large factorisation arises which represents the full statistical model under the assumption of additive white Gaussian noise.

There are two factorisations of (2) depicted in Figures 4 and 5. The first is used for estimating $\boldsymbol{\Theta}$ according to (7) (phase estimator in Fig. 3) and the second is used for estimating $\mathbf{A}$ according to (8) (coefficient estimator in Fig. 3).

In factor graphs edges represent variables and nodes represent factors. In this paper a factor is either (i) a hard constraint expressing the relationship between two or more variables or (ii) a prior probability density.

Messages are scaled conditional probability densities of the underlying edge, i.e. variable, arising as a result of summary propagation algorithms, in our case the sum-product rule. Messages can traverse the edges generally in both directions and are named μ including an arrow placed above it indicating the forward ($\overrightarrow{\mu}$) or backward ($\overleftarrow{\mu}$) direction with respect to the edge direction.

3.3 The Phase Estimator

The phase estimator makes use of a factor graph containing N consecutive sections one of which is depicted in Fig. 4. This means that the outgoing edge Θ_{n+1} of the graph in the figure is at the same time the incoming edge of its right neighbour.

The "Eq. (4)"-node represents the mathematical operation in (4).

There are two nodes connected to only one output

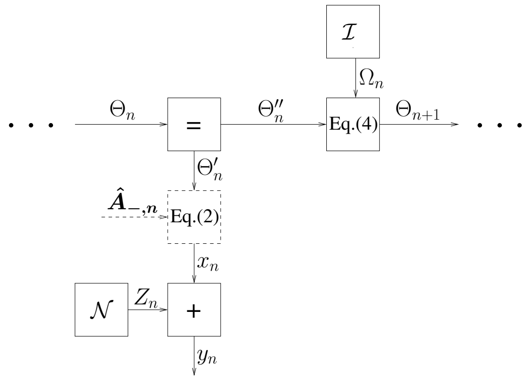

Figure 4: Factor graph used for estimation of the phase Θ_n.

and no input edges. The "$\mathcal{N}$"-node stands for zero-mean white Gaussian noise with variance σ^2, which is added to the clean sample x_n resulting in the observation sample y_n. The "$\mathcal{I}$"-node represents the prior knowledge about the upper and lower limits of the fundamental frequency, i.e. a density $I(\omega)$ with $\omega \in [0, 2\pi]$ which is uniform for $\omega \in [\Omega_{\min}, \Omega_{\max}]$ and 0 elsewhere, dictating that any growth of Θ_n outside the interval $[\Omega_{\min}, \Omega_{\max}]$ is invalid. Depending on the application and the prior knowledge, however, it might be advisable to replace the uniform distribution by a different probability distribution.

Taking the example of the arterial pulsation of humans, the rate of a regular heartbeat takes values between some minimum $H_{\min}$ and some maximum $H_{\max}$. Considering that the acquisition instruments measure with a sampling frequency f_s [Hz] and that during one heartbeat the phase traverses the interval $[0, 2\pi]$, each heart rate H can be assigned to an angle growth Ω according to

$$\Omega(H) = \frac{H \cdot 2\pi}{f_s \cdot 60}.$$

From given $H_{\min}$ and $H_{\max}$ the corresponding angle growth values $\Omega_{\min} = \Omega(H_{\min})$ and $\Omega_{\max} = \Omega(H_{\max})$ can be calculated.

The "="-node expresses cloning of the input variable Θ_n, thus Θ'_n and Θ''_n are clones of Θ_n.

The "Eq.(2)"-node represents the mathematical operation in (2) with $A_{k,n} = \hat{A}_{k,n}$ for $k = 0, \ldots, K$.

The schedule of the message passing algorithm on the phase estimator factor graph can be stated as follows:

1. For $n = 1, \ldots, N$, calculate $\overleftarrow{\mu}_{\Theta'_n}$ from the observation y_n.
2. For $n = 1, \ldots, N$, first calculate $\overrightarrow{\mu}_{\Theta''_n}$ from $\overrightarrow{\mu}_{\Theta_n}$ and $\overleftarrow{\mu}_{\Theta'_n}$, then calculate $\overrightarrow{\mu}_{\Theta_{n+1}}$ from $\overrightarrow{\mu}_{\Omega_n}$ and $\overrightarrow{\mu}_{\Theta''_n}$. There is no prior knowledge on Θ_1, thus the message $\overrightarrow{\mu}_{\Theta_1}$ is neutral: $\overrightarrow{\mu}_{\Theta_1}(\theta) = 1$ for all $\theta \in [0, 2\pi]$.
3. For $n = N, \ldots, 1$, first calculate $\overleftarrow{\mu}_{\Theta''_n}$ from $\overrightarrow{\mu}_{\Omega_n}$ and $\overleftarrow{\mu}_{\Theta_{n+1}}$, then calculate $\overleftarrow{\mu}_{\Theta_n}$ from $\overleftarrow{\mu}_{\Theta''_n}$ and $\overleftarrow{\mu}_{\Theta'_n}$. There is no prior knowledge on Θ_{N+1} (or Θ_N respectively), thus $\overleftarrow{\mu}_{\Theta_{N+1}}$ (or equivalently $\overleftarrow{\mu}_{\Theta''_N}$) is neutral: $\overleftarrow{\mu}_{\Theta_{N+1}}(\theta) = \overleftarrow{\mu}_{\Theta''_N}(\theta'') = 1$ for all $\theta, \theta'' \in [0, 2\pi]$.
4. For $n = 1, \ldots, N$, calculate the marginal $\tilde{\mu}_{\Theta''_n} = \overrightarrow{\mu}_{\Theta''_n} \cdot \overleftarrow{\mu}_{\Theta''_n}$.
5. For $n = 1, \ldots, N$, calculate the estimate $\hat{\Theta}_n = \underset{\theta_n}{\arg\max}\ \tilde{\mu}_{\Theta''_n}(\theta_n)$.

The messages on the Θ edges can in general not be described by a few parameters. Therefore the messages in the phase estimator are approximated by uniform discretisation.

It might seem more convincing to replace (7) with the vector estimate

$$\hat{\boldsymbol{\Theta}} = \underset{\boldsymbol{\Theta} \in [0, 2\pi]^N}{\arg\max}\ f\Big(\boldsymbol{\Theta}\ \Big|\ \boldsymbol{y}, \hat{\mathbf{A}}\Big).$$

This would lead to changing the sum-product rule to the max-product rule in the phase estimator. In the application with the arterial pulsation in humans measured with NIRS, however, we prefer the sum-product rule because the inherent averaging leads to less overfitting. The latter results from a large heart rate variability ($H_{min} \approx 60$ beats per minute and $H_{max} \approx 180$ beats per minute) implying a wide interval $[\Omega_{min}, \Omega_{max}]$ and thus a very soft constraint (5).

3.4 The Coefficient Estimator

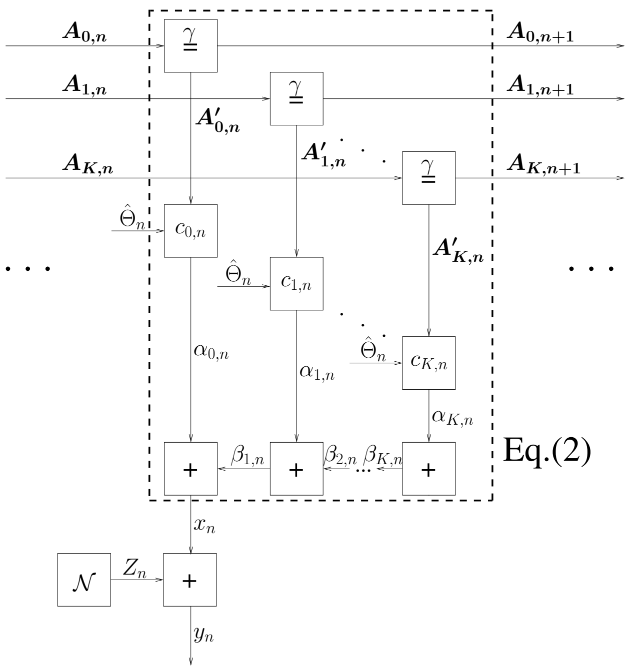

Figure 5: Factor graph used for estimation of the coefficient vector $\boldsymbol{A}_{-,n}$.

The coefficient estimator makes use of a factor graph containing N consecutive sections, one of which is depicted in Fig. 5. The arrangement of the sections is similar as described in 3.3.

The "$\overset{\gamma}{=}$"-node models a central property of almost periodic signals. It is equivalent with the "="-node with the additional feature that the significance of the message coming from the neighbour graph section is somewhat reduced before the summary proceeds. This is done by taking the message to the power of $\gamma \lesssim 1$ which we call "message damping" and which for Gaussian messages results in dividing the variance by γ. This clarifies (3) and allows variation of the coefficients from one discrete point in time to the next. During each further summarisation the variance of that message is divided by γ meaning that its significance is exponentially decaying with increasing distance to its original time index.

Furthermore there is the "$c_{k,n}$"-node, which maps some complex coefficient $A_{k,n}$ and phase Θ_n to the k-th harmonic part $\alpha_{k,n}$ of the almost periodic signal sample value x_n. Note that the k-th summand of the model equation (2) is

$$\begin{aligned} \alpha_{k,n} &\triangleq \mathrm{Re}(A_{k,n} \cdot e^{jk\Theta_n}) \\ &= \mathrm{Re}(A_{k,n}) \cdot \cos(k\Theta_n) + \mathrm{Im}(A_{k,n}) \cdot \sin(k\Theta_n) \\ &= \boldsymbol{A}_{k,n} \cdot \boldsymbol{c}_{k,n} \end{aligned} \tag{9}$$

with $\boldsymbol{A}_{k,n} \triangleq (\mathrm{Re}(A_{k,n}), \mathrm{Im}(A_{k,n}))$ and $\boldsymbol{c}_{k,n} \triangleq (\cos(k\Theta_n), \sin(k\Theta_n))^T$. The summation of all harmonics $\alpha_{k,n}$ for $k = 0, \ldots, K$ results in x_n.

Because Gaussian messages are used and gaussianity is preserved during summary propagation through all nodes in the factor graph in Fig. 5 ([2], Chapter V), two parameters, the covariance matrix $\mathbf{V}$ and the mean vector $\boldsymbol{m}$, suffice to describe any message in the graph.

The schedule of the message passing algorithm on the coefficient estimator factor graph can be formulated as follows:

1. Set $k = 0$.
2. For $n = 1, \ldots, N$, calculate sequentially the backward messages $\overleftarrow{\mu}_{x_n}$, $\overleftarrow{\mu}_{\alpha_{k,n}}$ and $\overleftarrow{\mu}_{\boldsymbol{A}'_{k,n}}$ from the observation y_n and estimate $\hat{\Theta}_n$, assuming $\beta_{k+1,n} = 0$ and $\alpha_{m,n} = \hat{\alpha}_{m,n}$ for $m = 0, 1, \ldots, k-1$.
3. For $n = 2, \ldots, N$, calculate $\overrightarrow{\mu}_{\boldsymbol{A}_{k,n}}$ from $\overrightarrow{\mu}_{\boldsymbol{A}_{k,n-1}}$ and $\overleftarrow{\mu}_{\boldsymbol{A}'_{k,n}}$. There is no prior knowledge on $A_{k,1}$, thus $\overrightarrow{\mu}_{\boldsymbol{A}_{k,1}}$ is neutral.
4. For $n = N, \ldots, 1$, calculate $\overleftarrow{\mu}_{\boldsymbol{A}_{k,n}}$ from $\overleftarrow{\mu}_{\boldsymbol{A}_{k,n+1}}$ and $\overleftarrow{\mu}_{\boldsymbol{A}'_{k,n}}$. There is no prior knowledge on $A_{k,N+1}$, thus $\overleftarrow{\mu}_{\boldsymbol{A}_{k,N+1}}$ is neutral.
5. For $n = 1, \ldots, N$, calculate $\overrightarrow{\mu}_{\boldsymbol{A}'_{k,n}}$ from $\overrightarrow{\mu}_{\boldsymbol{A}_{k,n}}$ and $\overleftarrow{\mu}_{\boldsymbol{A}_{k,n+1}}$.
6. For $n = 1, \ldots, N$, calculate the marginal $\tilde{\mu}_{\boldsymbol{A}'_{k,n}} = \overrightarrow{\mu}_{\boldsymbol{A}'_{k,n}} \cdot \overleftarrow{\mu}_{\boldsymbol{A}'_{k,n}}$ and the estimate $\hat{\boldsymbol{A}}_{k,n} = \underset{\boldsymbol{A}_{k,n}}{\arg\max}\ \tilde{\mu}_{\boldsymbol{A}'_{k,n}}(\boldsymbol{A}_{k,n})$.
7. For $n = 1, \ldots, N$, calculate $\hat{\alpha}_{k,n} = \hat{\boldsymbol{A}}_{k,n} \cdot \boldsymbol{c}_{k,n}$ according to (9).
8. If $k = K$ all coefficients have been estimated, stop the algorithm or else, increase k and continue on 2.

4. RESULTS AND CONCLUSION

Many signals in nature are almost periodic. In this paper, we propose a new approach to modelling such signals by means of Fourier series where both the coefficients and the fundamental frequency can continuously change over time. A factor graph representation of such models allows to estimate, with a complexity that is linear both in the number of frequencies K and in the observation length N, the time-dependent model parameters from noisy samples of the signal by means of message passing algorithms.

From a subjective point of view, the resulting estimates, shown in Fig. 2, are reasonable already after 3 iterations. We conclude that our approach has been successfully applied to NIRS and thus its usability is shown.

REFERENCES

[1] H.-A. Loeliger, "An introduction to factor graphs," *IEEE Signal Proc. Mag.,* Jan. 2004, pp. 28–41.

[2] H.-A. Loeliger, Justin Dauwels, Junli Hu, Sascha Korl, Li Ping and Frank R. Kschischang, "The factor graph approach to model-based signal processing," *Proc. of the IEEE,* June 2007, vol. 95, no. 6, pp. 1295–1322.

[3] A. Hyvärinen and E. Oja, "Independent component analysis: algorithms and applications", *Neural Networks,* 2000, vol. 13, no. 4–5, pp. 411–430.

[4] F. Scholkmann, *Signalverarbeitung in Bezug auf Untersuchung des Gehirns mit Licht: Entwicklung und Optimierung von Filtern und Charakterisierung von verschiedenen Signalkomponenten*, diploma thesis, University Hospital Zurich / FH Isny, 2007.

[5] D. V. Haensse, *Changes in Cerebral Oxygenation in Response to Various Stimuli in Newborns as Measured by Functional Near-Infrared Spectroscopy*, Ph.D. thesis at ETH Zurich No. 16356, Zurich 2006.

[6] M. Wolf, M. Ferrari, and V. Quaresima, "Progress of near-infrared spectroscopy and topography for brain and muscle clinical applications", *J. Biomed. Opt.* 12(6), 062104 (2007).

[7] S. Wray, M. Cope, D. T. Delpy, J. S. Wyatt, and E. O. Reynolds, "Characterization of the near-infrared absorption spectra of cytochrome aa3 and haemoglobin for the non-invasive monitoring of cerebral oxygenation," *Biochim. Biophys. Acta* 933(1), 184–192 (1988).

[8] H. Obrig, M. Neufang, R. Wenzel, M. Kohl, J. Steinbrink, K. Einhäupl, and A. Villringer, "Spontaneous Low Frequency Oscillations of Cerebral Hemodynamics and Metabolism in Human Adults," *NeuroImage,* Dec. 2000, Vol. 12, No. 6, pp. 623–639.